EUROPHYSICS LETTERS 15 September 2003

Europhys. Lett., **63** (6), pp. 833–839 (2003)

Wall thickness and core radius determination in surfactant templated silica thin films using GISAXS and X-ray reflectivity

A. Gibaud[1,3], A. Baptiste[1], D. A. Doshi[2], C. J. Brinker[2,3], L. Yang[4] and B. Ocko[4]

[1] *Université du Maine, Faculté des Sciences - 72085 Le Mans Cedex 09, France*
[2] *University of New Mexico - Albuquerque, NM 87106, USA*
[3] *Sandia National Laboratory - Albuquerque, NM 87185, USA*
[4] *Brookhaven National Laboratory - Upton Long Island, NY, 11987, USA*

(received 23 January 2003; accepted in final form 2 July 2003)

PACS. 61.10.Dp – Theories of diffraction and scattering.
PACS. 81.07.Bc – Nanocrystalline materials.
PACS. 68.35.Md – Surface thermodynamics, surface energies.

Abstract. – X-ray reflectometry and GISAXS (grazing angle small angle scattering) are combined to investigate the morphology and structural parameters of a surfactant templated 2D hexagonal thin-film silica mesophase. It is shown that X-ray reflectivity measurements contain invaluable information about the radius of the cylindrical rods and the distance between their cores. The reflectivity data are analyzed using a model of the electron density and combined with GISAXS measurements to derive the silica wall thickness.

Introduction. – Supramolecular-templating approach pioneered by Mobil researchers [1] uses surfactants to self-assemble inorganic precursors, such as that of silica, into precise arrangements of inorganic and organic constituents on the 1–50 nm length scale. Over the last 5 years, their synthesis has been adapted to the fabrication of supported inorganic mesoporous thin films using simple evaporation-induced self-assembly (EISA) [2] procedures such as dip-coating [3–7] and spin-coating [2, 8, 9]. Supported mesoporous inorganic thin-films are important for their applications in membranes [6], sensors [10, 11], photonics [12, 13], low dielectric constant insulators [14–17] and fluidic devices. Films with various morphologies: lamellar [3, 18], hexagonal [3, 4, 7], cubic [3–5, 19], 3D-hexagonal [3, 5, 20] have been fabricated, and techniques such as X-ray diffraction (XRD) [3, 4, 7], GISAXS [7, 9, 20, 21], scanning electron microscopy (SEM) [3], transmission electron microscopy (TEM) [3, 4, 20], atomic force microscopy (AFM) used to derive morphological and structural information. The structural dimensions of the organic and the inorganic phase dictate the final material properties such as mechanical strength, refractive index, dielectric constant, pore size, and surface area. Surface acoustic wave techniques combined with nitrogen adsorption [22, 23] have been used to characterize the pore size [3, 4] and in combination with X-ray data used to calculate the

© EDP Sciences

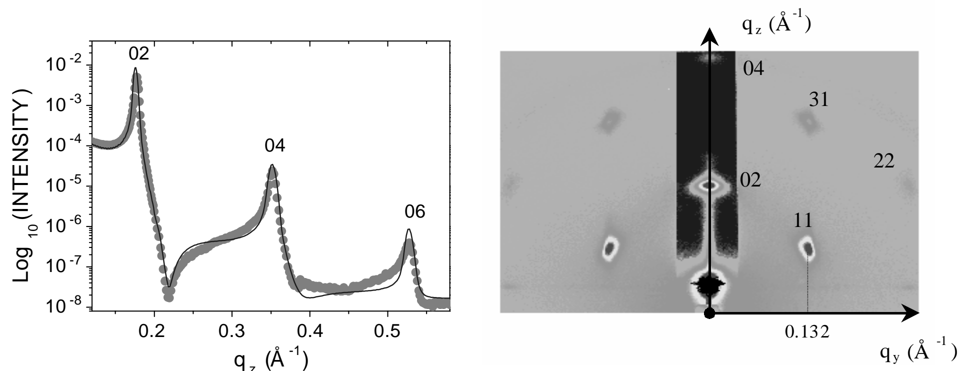

Fig. 1 – Left part: calculated (full line) and observed (open circles) X-ray reflectivity of a dry film showing the presence of Bragg peaks (indexed in the face-centered rectangular unit cell) and dips. Right part: GISAXS pattern of the mesophase thin film showing the distorted 2D hexagonal reciprocal lattice. The black dot close to the origin is the saturation at the silicon critical wave vector transfer. The central stripe is due to the attenuator. The scale is the same on both axes. Bragg reflections are indexed in the face-centered rectangular unit cell (*cmm*).

silica wall thickness [24] for films where the surfactant (organic phase) has been removed by solvent extraction [25], UV ozone [26], or heat treatment [3, 4, 7]. In thin films, non-evasive determination of the structural dimensions of the organic and inorganic phase, in particular of the wall thickness and pore size, is desirable for both technological and scientific reasons. Here, we present a new approach to non-evasively determine such parameters in surfactant templated silica thin-film.

Experimental. – Precursor solutions were prepared using a two-step procedure reported previously [3]. Final reactant mole ratios were 1TEOS : 20 C_2H_5OH : 5.1 H_20 : 0.0026 HCl : 0.16C_{16}TAB (cetyltrimethylammonium bromide). Evaporation accompanying film deposition by dip coating concentrates the depositing film in surfactant and silica inducing the self-assembly of micelles and their further organization into liquid-crystalline silica/surfactant mesophases. The effective initial solution pH ($-\log[H_3O^+]$) was 2, which largely precludes further siloxane condensation reactions accompanying EISA [2,27], thereby enabling self-assembly to proceed unimpeded. 300 μm thick Si (100) substrates were dip-coated at a withdrawal rate of 1.6 mm/s at 25 °C at 25% relative humidity.

X-ray experiments were performed at National Synchrotron Light Source, Brookhaven National Laboratory, USA. X-ray reflectivity measurements were performed at the X22A beam line with a 11 keV monochromatic beam. The incident and scattered beams were collimated so as to achieve a direct beam FWHM (full width at half-maximum) of 0.04°. Measurements were made in strictly specular conditions and were corrected by subtracting the longitudinal specular background which was found to be almost negligible. 2D GISAXS measurements were performed on the same sample at the X21 beam line to obtain the morphological information. A monochromatic beam, at an energy of 8.2 keV, impinged on the sample at an incident angle $\theta = 0.24°$ (slightly higher than the critical angle of silicon substrate). The scattered beam was monitored by a 2D MAR CCD detector located 1.2 m from the sample. The specular direction was attenuated in the vicinity of the critical angle to prevent detector saturation.

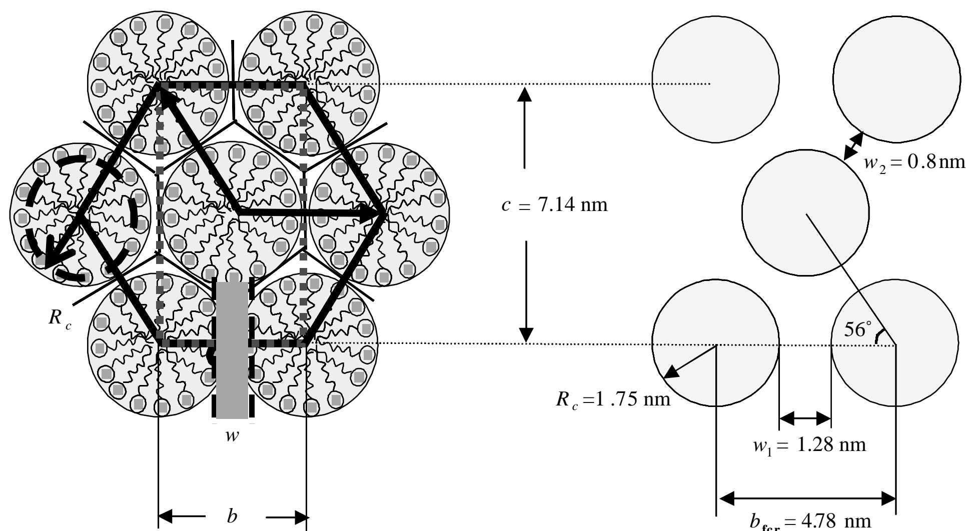

Fig. 2 – Left part: schematics of the 2D hexagonal mesophase structural arrangement showing the parameters reported in the text. The rectangular face-centered unit cell with lattice parameters b and c is indicated in dashed line. The inner radius of the cylindrical core is represented by an arrow. The silica wall thickness is highlighted. Right part: The real distorted lattice corresponding to the GISAXS pattern of fig. 1.

Results and discussion. – X-ray reflectivity (see left part of fig. 1) of C_{16}TAB templated thin-film silica mesophases deposited on a silicon wafer exhibits two characteristic features. As in 1D periodic structures, equally spaced intense Bragg peaks are observed along the q wave vector transfer (q_z) perpendicular to the plane of the substrate surface. The peak positions correspond to a characteristic period $\Lambda = 35.6$ Å.

More remarkable are the dips visible at q_z values higher than the one corresponding to the Bragg peaks. Such dips are sometimes observed in materials that have a thin top layer exhibiting a large electron density contrast with the rest of the structure [28]. However, GISAXS measurements (see right part of fig. 1) performed on the same film reveal a 2D hexagonal structure. The 2D mesophase consists of cylindrical rods organized on a hexagonal lattice with their axes oriented parallel to the substrate surface. The absence of a Bragg reflection at $q_y = 0.132$ Å^{-1} and $q_z = 0$ Å^{-1} rules out the possibility of a 3D hexagonal phase [20, 29].

The observation of this GISAXS pattern has a threefold consequence: i) since observed off-axis reflections are located at half the q_z position of the specular reflections, the period Λ found along q_z in the reflectivity curve is half of the true period; ii) due to the distortion of the initial 2D hexagonal lattice, the 2D lattice that describes the GISAXS pattern is a face-centered rectangular (FCR) lattice [7] with $a_{\mathrm{fcr}} = 4.78$ nm and $c_{\mathrm{fcr}} = 2\Lambda = 7.15$ nm as shown in fig. 2; iii) the dips are unlikely related to the presence of a thin high electron density layer at the top surface of the film, but more to the existence of nearly monodisperse rods of surfactant molecules templating the silica matrix. These closely packed rods have a form factor given by a first-order Bessel function that exhibits marked zeros. Here, the first zero is observed at $q_z = 0.217$ Å^{-1} and the next two are less marked at $q_z = 0.38$ Å^{-1} and $q_z = 0.56$ Å^{-1}. These positions correspond to rods of average radius 1.8 nm.

Quantitative information about the morphology of such films can be obtained through modelling the X-ray reflectivity curve. Since we have a periodic assembly of 2D mesoscopic objects, *i.e.* an inhomogeneous material at the wave vector transfer scale, it is not recommended to model the reflectivity within the framework of the dynamical theory. This theory is based on the reflection of X-rays by almost planar interfaces, and on representing the material as a set of homogeneous electron density slabs; these assumptions are not valid for a thin-film mesophase consisting of hexagonally packed cylindrical rods (or, alternatively, other kinds of objects). The Born approximation approach [30] allows the formulation of the reflectivity as a function of morphological parameters such as the radius, R, of the cylindrical rods and by the periodic distance, c, between the rods. This approximation can be used provided the scattered intensity is weak compared to that of the direct beam, *i.e.* far from the critical angle of external reflection.

Taking the origin of the z-axis at the silicon-film interface, we use a general approach in which the 2D electron density (ED), ρ, is formulated as the sum of three terms: the substrate ED, ρ_1, the average film ED, ρ_2, and the scattering objects ED, ρ_3. We have therefore

$$\rho(\vec{r}) = \rho_1(\vec{r}) + \rho_2(\vec{r}) + \rho_3(\vec{r}) \tag{1}$$

with

$$\begin{aligned}
\rho_1(\vec{r}) &= \rho_{\mathrm{Si}}\big(1-\theta(z)\big), \qquad \rho_2(\vec{r}) = \rho_m\big(\theta(z)-\theta(z-Mc-2R)\big),\\
\rho_3(\vec{r}) &= \big(\rho_{\mathrm{cyl}}(\vec{r})-\rho_m\big) * \delta(z-R) * \left(\delta(y)\delta(z)+\delta\left(y-\frac{b}{2}\right)\delta\left(z-\frac{c}{2}\right)\right) *\\
&\quad * \sum_{n=-\infty,m=1}^{n=\infty,m=M} \delta\left(\vec{r}-\vec{R}_{nm}\right),
\end{aligned}$$

where $\theta(z)$ is the Heaviside step function, $\vec{R}_{nm} = n\vec{b}+m\vec{c}$ is a vector joining two nodes of the direct lattice with b and c being the lattice parameters of the rectangular face-centered unit cell associated with the 2D hexagonal phase; ρ_{Si}, $\rho_{\mathrm{cyl}}(\vec{r})$, ρ_m the silicon, the hydrocarbon core of the cylindrical rods and the head group and silica host matrix electron densities. $\rho_3(\vec{r})$ was similarly described by [31] to analyze powder diffraction patterns of pluronic surfactants. Here we limit ourselves to a two-density-levels model to describe the thin-film morphology. More sophisticated models involving a corona of uniform electron density did not significantly improve the goodness of the fits [31]. Since we have a finite thickness, the sum over m in $\rho_3(\vec{r})$ runs only up to the total number, M, of rods coherently stacked in the z-direction. The Fourier transform of the three ED described by eq. (1) consists of three corresponding components:

$$\begin{aligned}
&F_1(q_y,q_z) = \frac{\rho_{\mathrm{Si}}}{-iq_z}2\pi\delta q_y, \qquad F_2(q_y,q_z) = 2\pi\rho_m\frac{e^{-iq_z(Mc+2R_{\mathrm{c}})}-1}{-iq_z}\delta q_y,\\
&F_3(q_y,q_z) = F_{\mathrm{cyl}}(\vec{q})\left(1+e^{-i\left(\frac{q_y b+q_z c}{2}\right)}\right)\frac{\sin\frac{q_z Mc}{2}}{\sin\frac{q_z c}{2}}\frac{2\pi}{b}e^{-iq_z\left(R_{\mathrm{c}}+(M-1)\frac{c}{2}\right)}\sum_n \delta\left(q_y-\frac{2\pi n}{b}\right),
\end{aligned} \tag{2}$$

with $F_{\mathrm{cyl}}(\vec{q}) = 2\pi R_{\mathrm{c}}^2 L(\rho_{\mathrm{cyl}}-\rho_m)\frac{J_1(qR_{\mathrm{c}})}{qR_{\mathrm{c}}}$ [31], where $q=\sqrt{q_y^2+q_z^2}$ and L is the length of the cylinder in the x-direction (note that since in the measurements we do not have access to this quantity, the quantity $L(\rho_{\mathrm{cyl}}-\rho_m)$ is replaced by a scale factor). The orientation of the

cylinders is considered here to be parallel to the x-direction. In the 2D hexagonal phase this statement is not true. The cylinders are randomly oriented in the xOy plane parallel to the surface of the film. This means that the q_x- and the q_y-dependence are coupled, but q_z remains independent. It is worth noting that F_1 and F_2 describe the contribution of the interfaces whereas F_3 is related to the distorted 2D Hex lattice and gives rise to Bragg scattering. In the Born approximation the specular reflectivity, R, which is solely dependent on the q_z wave vector component, relates directly to the Fourier transforms of the derivative of the electron density, and therefore to the Fourier transform of the electron density itself by

$$R(q_z) = \frac{R_{\mathrm{F}} q_z^2}{4\pi^2 A}\left|\frac{1}{\rho_{\mathrm{Si}}}\int \rho(z) e^{-iq_z z}\,\mathrm{d}z\right|^2 = R_{\mathrm{F}}\left|\frac{1}{\rho_{\mathrm{Si}}}\int \frac{\mathrm{d}\rho(z)}{\mathrm{d}z} e^{-iq_z z}\,\mathrm{d}z\right|^2, \tag{3}$$

where R_{F} is the Fresnel reflectivity of the bare silicon substrate, A is the illuminated area of the sample and $\int \rho(z)e^{-iq_z z}\,\mathrm{d}z = F_1(0,q_z) + F_2(0,q_z) + F_3(0,q_z)$. The measured reflectivity is the convolution of $R(q_z)$ with the resolution function of the instrument which was considered to be Gaussian-like with a HWHM of $0.002\,\text{Å}^{-1}$. In addition, thermal vibrations of the cylinders are taken in account by a Debye-Waller factor σ which smears out the higher-order Bragg reflections.

Flat interfaces and the long-range in-plane order present in a 2D hexagonal phase imposes the intensity to be located at the Bragg peak positions described by the delta-functions in the q_y direction contained in all the terms (F_1, F_2, F_3). This precludes the observation of any specific scattering in the off-axis direction except for the Bragg peaks located at $q_y = \frac{2\pi n}{b}$. However, this restriction does not apply to the specular direction making it the privileged direction to study the morphological properties of the mesophase. Along q_z the form factor of the cylindrical rods $F_{\mathrm{cyl}}(\vec{q})$ produces a dip in the reflectivity curve. The low polydispersity of the surfactant chain length translates to a low polydispersity in the surfactant rod diameters, and therefore an extremely pronounced dip is observed (fig. 1). The location of the dip is related to the first zero of the first-order Bessel function contained in $F_{\mathrm{cyl}}(\vec{q})$. This zero located at $q_z = 3.84/R_{\mathrm{c}}$ determines unambiguously the radius of the hydrocarbon core of the cylinders. For the film measured in fig. 1, the first dip is located at $q_z = 0.217\,\text{Å}^{-1}$ which yields $R_{\mathrm{c}} = 1.77\,\mathrm{nm}$. Within the context of the present model, the radius of the top layer dictates the asymmetry of the peaks and the radius of the other layers is determined by the relative intensity of the different peaks through the Bessel function term.

The electron density model described by eq. (1) is used to fit the reflectivity data in which a scale factor and the following parameters R_{c}, c, M, σ are allowed to vary. The calculated reflectivity shown in fig. 1 reproduces most of the observed features. It is found that the main contribution to the calculated reflectivity comes from the Bragg scattering term F_3. As $M = 25$, the film thickness is close to 180 nm and the Kiessig fringes that are contained in F_2 are not visible after convoluting $R(q_z)$ with the instrumental function.

The observed reflectivity agrees fairly well with the calculated one given the simplicity of our model which does not account for any kind of distortion of the lattice neither for any polydispersity. From the fit $M = 25$, $\sigma = 0.35\,\mathrm{nm}$, $c = 7.14 \pm 0.03\,\mathrm{nm}$ and $R_{\mathrm{c}} = 1.75 \pm 0.03\,\mathrm{nm}$. Since the persistence length of the surfactant aliphatic chain composed of 16 carbons is 2.04 nm we conclude, based on the measured radius, that the aliphatic chains are stretched to about 86% of their maximum all-trans length. The head group of the surfactant molecule has a higher electron density (presence of bromide) and its contribution is combined with that of the silica network. As shown in fig. 2, it is possible to estimate the silica wall thickness (together with the head of the surfactant molecule) from $b = b_{\mathrm{fcr}}$ and R_{c} since $w = b - 2R_{\mathrm{c}}$. In a perfect 2D hexagonal structure the distance between the cores of two cylinders should be

$a_{\rm hex} = b_{\rm fcr} = c_{\rm fcr}/\sqrt{3}$. For $c = 7.14\,{\rm nm}$, this yields $a_{\rm hex} = 4.13 \pm 0.03\,{\rm nm}$ and the wall thickness would be $0.63 \pm 0.09\,{\rm nm}$. This is without accounting for the shrinkage of the film in the direction perpendicular to the substrate surface. Simultaneous GISAXS measurements shown in fig. 1 enable us to probe the distortion of the lattice. The c lattice parameter which can be deduced from the GISAXS pattern is found to be in perfect agreement with the one derived from reflectivity analysis. In contrast, the observed b lattice parameter, $b = 4.78 \pm 0.03\,{\rm nm}$, is larger than the one calculated from $b_{\rm fcr} = c_{\rm fcr}/\sqrt{3}$. Assuming that the cylinders remain unaffected by the shrinkage of the lattice, the silica wall thickness becomes anisotropic (as shown in the right part of fig. 2). In the in-plane direction, the thickness is $w_1 = 1.28 \pm 0.09\,{\rm nm}$, whereas it is $w_2 = 0.8 \pm 0.09\,{\rm nm}$ at 56.2° of this direction. The in-plane value of the wall thickness compares well with estimates found in the literature [23]. Finally, it is worth noting that this approach is working well only if the scattering objects are quite monodispersed. For surfactant such as pluronic F127 and P123 that exhibit polydispersed shapes and produce similar 2D Hex structures, the absence of dips in the reflectivity curve is expected.

Conclusions. – We have shown in this paper that the combined quantitative analysis of X-ray reflectivity and GISAXS patterns can yield a precise determination of the cylindrical core radius together with the silica wall thickness of silica surfactant templated mesophases. The radius of the cylindrical cores is directly related to the observation of very pronounced dips in the X-ray reflectivity patterns, while the wall thickness can be non-evasively accessed from the knowledge of the lattice parameters of the 2D distorted hexagonal structure and form the radius of the core. More generally, our approach is applicable to any films presenting monodispersed objects periodically stacked in a host matrix provided the electron density of these objects is correctly described in eq. (2).

Similar measurements are now planned in the same samples before and after calcination to probe the influence of thermal annealing on the possible deformation of the cylindrical rods.

* * *

This work was partially supported by the French ACI "Nanostructure" under project No. 03-01, the UNM/NSF Center for Micro-Engineered Materials, the Defense Advanced Research Projects Agency, the DOE Basic Energy Sciences Program and SNL's Laboratory Directed R&D program. Research carried out in part at the National Synchrotron Light Source, Brookhaven National Laboratory, was supported by the US Department of Energy under Contract No. DE-AC02-98CH10886, Division of Materials Sciences and Division of Chemical Sciences. Sandia is a multiprogram laboratory operated by Sandia Corporation, a Lockheed Martin Company, for the United States Department of Energy under contract DE-AC04-94AL85000.

REFERENCES

[1] Kresge C. T., Leonowicz M. E., Roth W. J., Vartuli J. C. and Beck J. S., *Nature*, **359** (1992) 710.
[2] Brinker C. J., Lu Y. F., Sellinger A. and Fan H. Y., *Adv. Mater.*, **11** (1999) 579.
[3] Lu Y. F., Ganguli R., Drewien C. A., Anderson M. T., Brinker C. J., Gong W. L., Guo Y. X., Soyez H., Dunn B., Huang M. H. and Zink J. I., *Nature*, **389** (1997) 364.
[4] Doshi D. A., Huesing N. K., Lu M. C., Fan H. Y., Lu Y. F., SimmonsPotter K., Potter B. G., Hurd A. J. and Brinker C. J., *Science*, **290** (2000) 107.
[5] Zhao D. Y., Yang P. D., Margolese D. I., Chmelka B. F. and Stucky G. D., *Chem. Commun.* (1998) 2499.

[6] TSAI C. Y., TAM S. Y., LU Y. F. and BRINKER C. J., *J. Membrane Sci.*, **169** (2000) 255.
[7] KLOTZ M., ALBOUY P. A., AYRAL A., MENAGER C., GROSSO D., VANDERLEE A., CABUIL V., BABONNEAU F. and GUIZARD C., *Chem. Mater.*, **12** (2000) 1721.
[8] OGAWA M., *Chem. Commun.* (1996) 1149.
[9] BESSON S., RICOLLEAU C., GACOIN T., JACQUIOD C. and BOILOT J. P., *J. Phys. Chem. B*, **104** (2000) 12095.
[10] INNOCENZI P., MARTUCCI A., GUGLIELMI M., BEARZOTTI A., TRAVERSA E. and PIVIN J. C., *J. Eur. Ceramic Soc.*, **21** (2001) 1985.
[11] WIRNSBERGER G., SCOTT B. J. and STUCKY G. D., *Chem. Commun.* (2001) 119.
[12] YANG P. D., WIRNSBERGER G., HUANG H. C., CORDERO S. R., MCGEHEE M. D., SCOTT B., DENG T., WHITESIDES G. M., CHMELKA B. F., BURATTO S. K. and STUCKY G. D., *Science*, **287** (2000) 465.
[13] SCOTT B. J., WIRNSBERGER G. and STUCKY G. D., *Chem. Mater.*, **13** (2001) 3140.
[14] FAN H. Y., BENTLEY H. R., KATHAN K. R., CLEM P., LU Y. F. and BRINKER C. J., *J. Non-Cryst. Solids*, **285** (2001) 79.
[15] BASKARAN S., LIU J., DOMANSKY K., KOHLER N., LI X. H., COYLE C., FRYXELL G. E., THEVUTHASAN S. and WILLIFORD R. E., *Adv. Mater.*, **12** (2000) 291.
[16] SERAJI S., WU Y., FORBESS M., LIMMER S. J., CHOU T. and CAO G. Z., *Adv. Mater.*, **12** (2000) 1695.
[17] YANG C. M., CHO A. T., PAN F. M., TSAI T. G. and CHAO K. J., *Adv. Mater.*, **13** (2001) 1099.
[18] HUANG M. H., DUNN B. S., SOYEZ H. and ZINK J. I., *Langmuir*, **14** (1998) 7331.
[19] GROSSO D., BABONNEAU F., ILLIA G. J. D. A., ALBOUY P. A. and AMENITSCH H., *Chem. Commun.* (2002) 748.
[20] GROSSO D., BALKENENDE A. R., ALBOUY P. A., LAVERGNE M., MAZEROLLES L. and BABONNEAU F., *J. Mater. Chem.*, **10** (2000) 2085.
[21] GROSSO D., BABONNEAU F., ALBOUY P. A., AMENITSCH H., BALKENENDE A. R., BRUNEAU A. and RIVORY J., *Chem. Mater.*, **14** (2002) 931.
[22] FRYE G. C., RICCO A. J., MARTIN S. J. and BRINKER C. J., *Mater. Res. Soc. Symp. Proc.*, **121** (1988) 349.
[23] GALARNEAU A., DESPLANTIER D., DUTARTRE R. and DI RENZO F., *Langmuir*, **17** (2001) 8328.
[24] FAN H. Y., PhD Dissertation, Department of Chemical, Nuclear Engineering, University of New Mexico (2000).
[25] GROSSO D., BALKENENDE A. R., ALBOUY P. A., AYRAL A., AMENITSCH H. and BABONNEAU F., *Chem. Mater.*, **13** (2001) 1848.
[26] CLARK T., RUIZ J. D., FAN H. Y., BRINKER C. J., SWANSON B. I. and PARIKH A. N., *Chem. Mater.*, **12** (2000) 3879.
[27] BRINKER C. J. and SCHERER G. W., *Sol-Gel Science: The Physics and Chemistry of Sol-Gel Processing* (Academic Press) 1990.
[28] CHU S., YONG, ROBINSON I. K. and GEWIRTH A. A., *Phys. Rev. B*, **55** (1997) 7945.
[29] GROSSO D., ALBOUY P. A., AMENITSCH H., BALKENENDE A. R. and BABONNEAU F., *Mater. Res. Soc. Symp. Proc.*, **628** (2000) CC6.17.1; CC6.17.7.
[30] GIBAUD A., HAZRA S., SELLA C., LAFFEZ P., DESERT A., NAUDON A. and VAN TENDELOO G., *Phys. Rev. B*, **63** (2001) 193407.
[31] IMPEROR-CLERC M., DAVIDSON P. and DAVIDSON A., *J. Am. Chem. Soc.*, **122** (2000) 11925.